

Monitoring of IR Clear-sky Radiances over Oceans for SST (MICROS)

Xingming Liang^{1,2*} and Alexander Ignatov¹

¹*NOAA/NESDIS, Center for Satellite Application and Research (STAR), Camp Springs, MD 20746*

²*Cooperative Institute for Research in the Atmospheres (CIRA), CSU, Fort Collins, CO 80523*

October 29, 2010

Abstract

Monitoring of IR Clear-sky Radiances over Oceans for SST (MICROS, www.star.nesdis.noaa.gov/sod/sst/micros/) is a Web-based tool to monitor “model minus observation” (M-O) biases in clear-sky brightness temperatures (BT) and sea surface temperatures (SST) produced by the Advanced Clear-Sky Processor for Oceans (ACSPO). Currently, MICROS monitors M-O biases in three AVHRR bands centered at 3.7, 11, and 12 μm for five satellites, NOAA-16, -17, 18, -19 and MetOp-A. The fast Community Radiative Transfer Model (CRTM) is employed to simulate clear-sky BTs, using Reynolds SST and National Centers for Environmental Prediction Global Forecast System profiles as input. The key MICROS objectives are to fully understand and reconcile CRTM and AVHRR BTs, and to minimize cross-platform biases through improvements to ACSPO algorithms, CRTM and its inputs, satellite radiances, and skin-bulk and diurnal SST modeling.

Initially, MICROS was intended for internal use within the NESDIS SST team for testing and improving ACSPO products. However, it has quickly outgrown this initial objective and is now used by several other research and applications groups. In particular, inclusion of double differences in MICROS has contributed to sensor-to-sensor

* *Corresponding author address: Xingming Liang, NOAA/NESDIS/STAR, WWB Rm. 603, 5200 Auth Rd, Camp Springs, MD 20746; e-mail: Xingming.Liang@noaa.gov*

monitoring within the Global Space-based Inter-Calibration System, which is customarily performed using the well established simultaneous nadir overpass technique. Also, CRTM scientists have made a number of critical improvements to CRTM using MICROS results. They now routinely use MICROS to continuously monitor M-O biases and validate and improve CRTM performance. MICROS is also instrumental in evaluating accuracy of the first guess SST and upper air fields used as input to CRTM. This paper gives examples of these applications and discusses ongoing work and future plans.

1. Introduction

Developed at the National Environmental Satellite, Data and Information Service (NESDIS), the Advanced Clear-Sky Processor for Oceans (ACSPO) became operational in May 2008 with the Global Area Coverage (GAC) data of the Advanced Very High Resolution Radiometers (AVHRR). As of this writing, ACSPO operational products are generated from NOAA-19 and Metop-A. Data from back-up satellites NOAA-16, -17 and -18 are also processed and used in MICROS for cross-platform consistency analyses.

The major ACSPO product is clear-sky radiances over ocean in all AVHRR bands. Sea surfaces temperatures (SST) are derived from clear-sky brightness temperatures (BT) in Ch3B (centered at 3.7 μm), Ch4 (11 μm), and Ch5 (12 μm), and aerosol optical depths are retrieved from clear-sky reflectances in Ch1 (0.63 μm), Ch2 (0.83 μm), and Ch3A (1.61 μm). All three products require validation against known reference data. In ACSPO, expected clear-sky BTs are simulated using the fast Community Radiative Transfer Model (CRTM) (*Han et al.*, 2006), similar to the RTM for TIROS operational vertical sounder

(RTTOV) (*Saunders et al.*, 1999). Reynolds daily SST (*Reynolds et al.*, 2007) and National Centers for Environmental Prediction (NCEP) Global Forecast System (GFS) upper air fields are used as input. CRTM BTs are used in ACSPO in conjunction with measured BTs for clear-sky masking (*Petrenko et al.*, 2010a) and for exploring improved SST retrievals (*Petrenko et al.*, 2010b). These applications require close agreement between modeled and observed BTs.

CRTM was implemented in ACSPO and preliminarily validated against AVHRR BTs, using one week of nighttime data (*Liang et al.*, 2009). In this initial implementation, model minus observation (M-O) global biases reached several kelvins. Substantial effort was invested into minimizing these large biases. As a result, in ACSPO version 1, implemented into NESDIS operations in May 2008, all M-O biases were reduced to only several tenths of a Kelvin and are now consistent across platforms to within $\sim 0.1\text{K}$. Note that slightly positive bias in the “M” is expected, due to missing aerosols in CRTM and using bulk (rather than cooler skin) Reynolds SST—which is not corrected for the effect of diurnal cycle—as input to CRTM. Also, residual cloud in the AVHRR clear-sky BTs decreases the “O” term, further amplifying positive shift in the M-O bias.

Customarily, empirical bias correction is performed to reconcile satellite and RTM radiances (e.g., *Uddström and McMillin*, 1994; *Harris and Kelly*, 2001; *Garand*, 2003; *Köpken et al.*, 2004; *Munro et al.*, 2004; *Merchant et al.*, 2008, 2009). Empirical bias correction is also employed in ACSPO (*Petrenko et al.*, 2010a, 2010b). However, this approach does not address the root causes of the bias, which may result from deficiencies

in CRTM or its inputs or errors in sensor calibration and spectral responses. To fully realize CRTM potential in ACSPO and reduce the need for, and reliance upon, the empirical bias correction, M-O biases should be constantly monitored, understood, and minimized based on first principles.

Towards this objective, a Web-based diagnostic tool, Monitoring of IR Clear-sky Radiances over Oceans for SST (MICROS, www.star.nesdis.noaa.gov/sod/sst/micros/) was established to evaluate the M-O BT and “regression minus Reynolds” SST biases in the ACSPO products, in near-real time. The MICROS system is described in section 2. Sections 3, 4, and 5 give examples of using MICROS for various applications. Section 6 concludes the paper and discusses ongoing work and future plans.

2. MICROS

2.1. The major premises of MICROS

In MICROS, differences between observations and their first guesses are monitored. Similar monitoring of M-O biases has been extensively used, for instance, in operational satellite data assimilation in European Centre for Medium-Range Weather Forecasts (ECMWF, www.ecmwf.int/products/forecasts/d/charts/monitoring/satellite/).

In the climate community, using anomalies (i.e., deviation of observation from the expected state) is known to reduce dependency on the non-uniform sample. If first-guess SST and GFS fields are close to reality and CRTM is accurate, then SST and BT biases should be small and characterized by near-Gaussian distribution (*Liang et al., 2009; Dash*

et al., 2010). For accurate cloud masking and SST retrievals in ACSPO, the model should closely match observations. However, non-zero M-O biases of several tenths of a kelvin persist in all AVHRR channels, with corresponding global standard deviations, $SD \sim 0.4\text{--}0.6\text{K}$ (*Liang et al.*, 2009).

In MICROS, statistical analyses of BT and SST biases are performed in the full clear-sky domain, including the full AVHRR swath $\pm 68^\circ$, and all results are displayed, with no exemption or additional quality control other than the ACSPO clear-sky mask (*Petrenko et al.*, 2010a). Biases are monitored in MICROS in several different ways:

- 1) Global maps of $\Delta T_B = BT_{\text{CRTM}} - BT_{\text{AVHRR}}$ and $\Delta T_S = SST_{\text{AVHRR}} - SST_{\text{Reynolds}}$ calculated and displayed, along with maps of corresponding geophysical and environmental parameters (water vapor, wind speed, Reynolds SST, air-sea temperature difference, and view and glint angles);
- 2) Histograms of BT and SST biases overlaid for five platforms with their summary daily statistics superimposed (number of observations, mean, SD);
- 3) Time series of global daily mean and SD statistics, along with double differences to evaluate the BT and SST biases for cross-platform consistency;
- 4) Dependencies on the main factors affecting the BT and SST biases: column water vapor content, view zenith angle, wind speed, Reynolds SST, air-sea temperature difference, and latitude.

In addition to conventional statistics (mean and SD) that are indicative of the overall performance of the ACSPO product, robust statistics (median and robust standard deviation, RSD) are also calculated to minimize the effect of possible outliers in ACSPO

data on the statistics (cf., *Merchant et al.*, 2008). Outlier-free statistics are particularly useful for validating CRTM and monitoring sensor radiances. Typically, the two statistics closely match, but occasionally they diverge, signaling problems with ACSPO products.

Examples are discussed in upcoming sections; more discussion of the monitoring principles is found in *Dash et al.* (2010), which documents another global monitoring system: the SST Quality Monitor (SQUAM; www.star.nesdis.noaa.gov/sod/sst/squam/).

2.2. Technical implementation

A flow chart of the MICROS system is shown in Fig. 1. MICROS employs ACSPO to process Level 1B data and generate product granules, which contain AVHRR and CRTM BTs, retrieved and Reynolds SSTs, cloud mask, solar and sensor view geometries, and additional ancillary data. Once ACSPO 1hr GAC granules have been generated, they are statistically processed in 24hr increments, and results are displayed on the Web. MICROS runs daily and processes global GAC data from five platforms (NOAA-16 to -19 and Metop-A). The end-to-end processing takes ~4 hours of clock time on a Linux box with four 2.33 GHz processors and 4 GB memory.

All analyses in MICROS are performed separately for day and night. As of this writing, nighttime analyses are more accurate and, therefore, more appropriate for validation of CRTM and satellite radiances, whereas daytime data are less accurate due to suboptimal treatment of solar reflection in CRTM v1.1 (*Liang et al.*, 2010). All analyses in this paper are based solely on nighttime ACSPO data.

3. Using MICROS to validate and improve ACSPO products

Since MICROS implementation in July 2008, it proved instrumental to evaluate and test all new ACSPO developments, in near-real time. This section documents results of testing three earlier ACSPO versions, which provided a natural way to estimate the stability and improvements in the ACSPO BT and SST biases.

3.1. ACSPO versions documented in MICROS

Three ACSPO versions are summarized in Table 1. ACSPO v1.00 was described in detail in (Liang *et al.*, 2009). It employed an alpha version of CRTM (termed “r577”) in conjunction with Reynolds weekly 1° SST (OISST.v2; Reynolds *et al.*, 2002) and an initial version of ACSPO cloud mask (Petrenko *et al.*, 2008).

In ACSPO v1.02, implemented in MICROS on 4 September 2008, three critical changes were made. First, weekly 1° Reynolds OISST.v2 was replaced with a more accurate daily 0.25° product (Reynolds *et al.*, 2007), which is based on blending Naval Oceanographic Office (NAVOCEANO) AVHRR SST product (May *et al.*, 1998) with *in situ* SST. Hereafter, this product is termed “Reynolds daily (AVHRR).” Another Reynolds daily product that additionally uses SST data from the Advanced Microwave Scanning Radiometer (AMSR) onboard *Aqua* satellite was also tested but did not show improvements in the BT and SST biases. Another critical update in ACSPO v1.02 was replacing CRTM r577 with the official CRTM version 1.1. Finally, the more accurate transmittance coefficient data for the wide AVHRR bands were used—referred to as

“Planck-weighted” coefficients (e.g., Chou *et al.*, 1993; Turner, 2000)—instead of the “ordinary” coefficients employed in CRTM r577.

ACSPO v1.10 was implemented on 3 January 2009. It employed improved clear-sky detection by using flexible band and sensor-specific tests (Petrenko *et al.*, 2010a). Also, the threshold at which the day/night flag switches over was changed from the solar zenith angle $SZA=85^\circ$ (in ACSPO v1.00 and 1.02) to $SZA=90^\circ$ (in v1.10).

In this section, we focus on evaluating the effect of these changes on global BT and SST biases. Also, out-of-family behavior of NOAA-16 is discussed in section 3.6.

3.2. Effect of using Daily Reynolds SST as CRTM input

Fig. 2 (a-b) shows that using more accurate daily SST reduces global variance (square of SD) of ΔT_B by half, and corresponding reduction is also observed in ΔT_S (not shown). Importantly, cross-platform consistency of BT and SST biases is also improved. A warm shift of $\sim +0.08$ K in BTs is due to an offset between weekly and daily Reynolds products on 12 July 2008, and a corresponding cold shift is observed in the “retrieved minus Reynolds SST” (not shown). Note that although both weekly and daily Reynolds SST products are anchored to *in situ* SST, small differences between them are possible, especially at the “end of period” for the weekly product (which is centered on Wednesdays; note that 12 July 2008 was a Saturday.) Fig. 3 (a-b) shows that the improvements in the M-O bias are more noticeable in higher latitudes and in some coastal areas. Although more stable and spatially coherent ΔT_B should favorably affect ACSPO

cloud mask, Figs. 2 and 3 (a-b) suggest that the clear-sky ocean domain did not change much, indicating that the ACSPO mask is robust with respect to first-guess SST field. Fig. 4 (a-b) additionally shows that the amplitude of the VZA dependencies remains largely unchanged. However, it is important to note that different platforms are clustered together more tightly now, likely due to reduced spatial and temporal noise in the higher resolution daily ($1 \text{ day} \times 0.25^\circ$) product compared to its weekly ($1 \text{ week} \times 1^\circ$) predecessor.

3.3. Effect of CRTM updates on ACSPO BTs

Figs. 2–4 (c) show the same data set as in Figs. 2–4 (b) but are processed with the new CRTM v1.1 formulation together with Planck-weighted coefficients. For this sensitivity check, the same daily Reynolds SST was used. The clear-sky coverage slightly increases, as is manifested by the larger N values in Fig. 2 (c). The mean ΔT_B biases are now reduced by $\sim -0.08 \text{ K}$, thus offsetting the positive shift of $\sim +0.08 \text{ K}$ that occurred as a result of using daily SST. The SDs did not change much. Additional analyses suggest that this change in CRTM BTs is mainly due to using Planck-weighted instead of ordinary coefficients.

Change from CRTM r577 to v1.1 affected NOAA-16 Ch3B in a very unique way, which was subject of a separate analysis (Liu *et al.*, 2009). Based on this analysis, treatment of upper atmospheric layers above 10 mbar in CRTM was revisited. As a result, the M-O bias in NOAA-16 Ch3B has increased by $\sim +0.3 \text{ K}$, and the corresponding SD significantly improved.

3.4. Effect of improved clear-sky mask on ACSPO BTs

The data set used in Figs. 2–4 (c) was processed using ACSPO v1.10, and results are shown in Figs. 2–4 (d). Compared to v1.02, the number of clear-sky observations at night has significantly reduced, mainly due to the change in day/night threshold in ACSPO v1.10, from $SZA=85^\circ$ to $SZA=90^\circ$. This reduction is only partly compensated by the increase in the daytime sample size, due to the additional updates in the cloud mask (Petrenko *et al.*, 2010a). Global mean BT and SST biases and their corresponding SDs have consistently reduced in ACSPO v1.10, and so did the amplitudes of their VZA dependencies, indicating that changes in the ACSPO clear-sky mask had favorable impact on the clear-sky BTs and SSTs from all platforms, except NOAA-16.

3.5. Time series of BT and SST biases

Time series of the mean BT and SST biases are shown in the left panels of Fig. 5. NOAA-19, launched on 6 February 2009, was added to MICROS monitoring on 23 February 2009, as soon as its thermal bands were commissioned and declared operational. On average, BT biases are $\sim+0.2$ K in Ch3B and $\sim+0.5$ K in Ch4 and Ch5. Physical mechanisms causing these warm biases were discussed in Liang *et al.* (2009) and reiterated above in section 1. There was no significant change in the mean M-O bias in any band of any platform (except NOAA-16 Ch3B) when the ACSPO version was upgraded from v1.00 to v1.02. This apparent lack of sensitivity is, in fact, due to compensation between two factors that offset each other: using daily Reynolds ($\sim+0.08$ K) and PW CRTM coefficients (~-0.08 K). Also, the BT and SST biases did not change

noticeably when ACSPO v1.10 was introduced, a remarkable result considering a significant adjustment in the ACSPO cloud mask (*Petrenko et al., 2010a*).

Contrary to the warm bias in ΔT_B , retrieved SSTs are biased cold with respect to Reynolds SST by several tenths of a kelvin (Fig. 5, g). Since Reynolds SST is anchored to *in situ* SSTs (*Reynolds et al., 2007*), global mean “ACSPO minus Reynolds SST” bias is a close proxy for the “ACSPO minus *in situ* SST” bias. To explain this cold bias in ACSPO SST, recall that coefficients of the regression algorithm are calculated against *in situ* SST using a training data set, and average bias between the two data sets is forced to zero. In the initial ACSPO versions discussed here, the SST formulation was intentionally preserved from the NESDIS heritage SST system, Main Unit Task (MUT) (*McClain et al., 1985; Ignatov et al., 2004*), for quick cross-evaluation of the two SST products. At night, the following triple-window Multi-Channel SST (MCSST) equation is employed:

$$T_s = a_0 + a_1 T_{3b} + a_2 T_4 + a_3 T_5 + [a_4 (T_{3b} - T_5) + a_5] (\sec \theta - 1) \quad (1)$$

The SST coefficients (a_0, a_1, a_2, a_3, a_4 , and a_5) in ACSPO have been adopted from MUT without change (*Dash et al., 2010*). However, nighttime BTs in MUT are biased warm with respect to ACSPO BTs because MUT selects the warmest clear-sky AVHRR pixel within a collocated High-Resolution Infrared Radiation Sounder (HIRS) footprint, whereas ACSPO processes all clear-sky pixels and does not subsample. Deriving coefficients against “warm-biased” MUT BTs, and using them in an “all clear-sky pixels”

ACSPO system, results in cold-biased ACSPO SSTs. Note that the SST Quality Monitor page

(www.star.nesdis.noaa.gov/sod/sst/squam/ACSPO/acsपो_pixel_level_timeseries.htm),

also shows a cold bias in nighttime ACSPO SSTs.

The right panels of Fig. 5 show corresponding global SDs. Unlike the global mean biases, the SDs of both ΔT_B and ΔT_S were significantly reduced (to 0.5 K in SST and Ch3B, 0.55 K in Ch4, and 0.65 K in Ch5) when ACSPO was upgraded from v1.00 to v1.02. This is mainly due to using a more accurate daily SST field instead of weekly. Recall also that Reynolds SSTs are analysis products (not forecast) and therefore are available in ACSPO in a delayed mode (the next day for the daily product, and the next week for the weekly).

To better understand the improvement from ACSPO v1.00 to v1.02, the plots from 1 July to 11 November 2008 are zoomed and superimposed in the upper-right of the corresponding panels. Note that each point now represents one day and not smoothed over seven days to preserve the fine temporal structure. Before 4 September 2008, the global SDs showed a prominent weekly cycle, largest in SST, followed by the most transparent Ch3B and then by Ch4 and Ch5. The corresponding cycles were also observed in the mean ΔT_B and ΔT_S biases (not shown), although they are seen less clearly than in the SDs. This periodicity was an artifact of using weekly Reynolds SST in ACSPO v1.00, which was resolved when daily SST was employed in ACSPO v1.02.

3.6. Anomalous behavior of NOAA-16

NOAA-16 biases are unstable, in all bands. Recall that this platform currently flies close to the terminator and its AVHRR black body experiences significant impingement from the solar radiation (*Cao et al.*, 2001; 2004a). This affects calibration in all AVHRR bands, with the largest effect expected in Ch3B. The AVHRR sensor on NOAA-16 had also experienced continuous problems since September 2003 and has not been used in NOAA operations after NOAA-18 was launched in May 2005.

In addition to the degraded orbit and unstable sensor, NOAA-16 Ch3B has shown a consistent cold bias of ~ -0.3 K with respect to several AVHRR instruments onboard other platforms (*Dash and Ignatov*, 2008; *Liang et al.*, 2009). This anomaly was analyzed in *Liu et al.* (2009) and found to be due to out-of-band leak in its spectral response function, which was incorrectly treated in CRTM r577. This problem was fixed in CRTM v1.1.

Despite these known problems with NOAA-16, we have opted to include it in the MICROS monitoring to better understand the performance of the ACSPO system in atypical situations. We believe that NOAA-16 problems may be corrected. Work with NESDIS calibration colleagues is underway to better understand root causes and to try to mitigate the problems. The current anomalous results will be used as a benchmark to measure future improvements. In the remainder of this paper, NOAA-16 results will be shown, for consistency, but not discussed pending future resolution of its data problems.

Overall, analyses in this section suggest that all the performance metrics employed in MICROS consistently improved with ACSPO versions.

4. Using MICROS to monitor sensor performance

Global mean biases in Fig. 5 experience day-to-day noise and long-term excursions. These artifacts are coherent between SST and all AVHRR bands, and for all platforms. Section 5 shows that they are caused by spurious variations in Reynolds SST, whose variations have the largest amplitude, followed by the most transparent Ch3B and then by Ch4 and Ch5. Note, for instance, a strong bump in $\Delta T_B \sim 0.3$ K in Ch3B and ~ 0.2 K in Ch4 and Ch5 in mid-April 2009, and several smaller bumps in early January and mid-October 2009. For each BT bump, there is a corresponding hump in ΔT_S .

Overall, BT biases show high degrees of stability and cross-platform consistency, suggesting that calibration and spectral response functions are relatively stable in time. However, spurious variability in data hinders accurate quantitative analyses of the platform-to-platform bias. In MICROS, a double-differencing (DD) technique was adopted to distinguish the cross-platform signal from noise. One platform is designated as “reference” (REF), and satellite-to-satellite BT and SST DDs are defined as follows:

$$SAT - REF = SAT[-(M - O)] - REF[-(M - O)] \quad (2)$$

$$SST - REF = SST[REG - REYNOLDS] - REF[REG - REYNOLDS] \quad (3)$$

The DD technique has been extensively employed, for instance, to establish a calibration link between the Atmospheric Infrared Sounder (AIRS) and the Infrared Atmospheric Sounding Interferometer (IASI) sensors using GOES (*Wang et al.*, 2008) or radiative transfer model simulation (*Strow et al.*, 2008) as a transfer standard, and to establish inter-calibration links between the *Terra* and *Aqua* MODIS instruments using AVHRR/NOAA-17 as a reference (*Wu et al.*, 2008). Similarly to the *Strow et al.* (2008) study, CRTM is used in MICROS as a transfer standard. The DD technique minimizes the effects on the BT artifacts that arise from such factors as errors in reference SST or in the GFS upper air data, incomplete inputs to CRTM (such as missing aerosol), possible systemic biases in the CRTM forward model, and updates in ACSPO processing algorithms. Furthermore, the effects of all these factors may change in time. The DD largely cancels out these unknown, uncertain, or unstable factors and is, thus, expected to be more effective to cross-calibrate different sensors.

Fig. 6 (left) shows DDs calculated from the corresponding panels in Fig. 5. NOAA-17 was used as a reference platform. Note that in contrast with the classical application of the DD technique, in MICROS the satellite footprints in the two data sets are not required to be co-located in space and time. The different clear-sky coverage between the two platforms likely contributes to day-to-day noise, but the effect of sampling largely cancels out, due to using BT and SST biases (i.e., differences rather than absolute values) in calculating DDs. The time series are further disturbed by other data issues, such as outliers and other gross data errors (e.g., present in NOAA-16). The right panels of Fig. 6 re-plot the left panels, but using median statistics. In all cases, median time series are less

noisy (cf. sigma values superimposed in the panels). Using robust statistics is thus preferred for DD analyses, whose objective is to rectify the cross-platform consistency signal while minimizing data noise. Note also that all data in Fig. 6 are additionally smoothed by a seven-day moving averaging filter, to further suppress noise in the data and rectify cross-platform signal.

Three flat lines represent the mean DD biases to help emphasize cross-platform consistency. NOAA-17 and Metop-A fly in close orbits (both cross the equator at ~21:30 local time). It is, therefore, not surprising to see that their ΔT_B 's are consistent to within several hundredths of a kelvin, in all bands. However, agreement between NOAA-17, on the one hand, and NOAA-18 and -19, on the other, is generally worse. Recall that the two latter “afternoon” satellites cross the equator close to ~1:40 a.m. and ~2 a.m. Typically, diurnal cooling in SST between 21 p.m. to 2 a.m. does not exceed ~0.1 K (e.g., *Garand, 2003; Stuart-Menteth et al., 2005; Kennedy et al., 2007; Gentemann and Minnett, 2008*). Nighttime BT biases in all bands and from all platforms are thus expected to be within several hundredths of a kelvin, somewhat larger in the transparent Ch3B and smaller in the more opaque Ch4 and Ch5. Clearly, the different bands of NOAA-18 and NOAA-19 do not follow this expected pattern, suggesting that their spectral response functions likely deviate from those assumed in the CRTM or that the calibration is off. Interestingly, cross-platform biases between NOAA-18 and NOAA-19 (0.09 K in Ch3B, 0.04 K in Ch4, and 0.12 K in Ch5) are quite large, although these platforms fly in close orbits. The DDs are also helpful to better quantify the instability in all bands of NOAA-16.

Note also that despite good consistency between BTs for Metop-A and NOAA-17, their corresponding SSTs significantly differ (by ~ 0.09 K). This is likely due to suboptimal specification of the regression coefficients in the NESDIS heritage MUT system, which are used “as is” in ACSPO.

The SDs of the DDs, σ , are also listed in Fig. 6. They can be used to estimate the uncertainties of the respective mean DDs. The standard error of the mean of an ensemble of N measurements is σ/\sqrt{N} . The time series in Fig. 6 span ~ 420 days, but the number of independent observations is effectively reduced to $N \sim 60$, due to seven-day averaging. For instance, standard error of the Metop-A minus NOAA-17 bias in Ch4 is $0.012K/\sqrt{60} \sim 0.0015$ K. The mean DD bias of -0.048 K thus appears statistically significant well beyond a 99% confidence level ($\pm 3\sigma_e$). These estimates demonstrate the accuracy potential of the DD technique to estimate cross-platform BT and SST biases.

It is useful to place the DD technique in context of the simultaneous nadir overpasses (SNO; www.star.nesdis.noaa.gov/smcd/spb/calibration/sno) technique (Cao *et al.*, 2004b; Tobin, 2008), adopted within the Global Space-based Inter-Calibration System (GSICS; www.star.nesdis.noaa.gov/smcd/spb/calibration/icvs/GSICS/index.php). In MICROS, cross-platform consistency is monitored in the full global domain and in the full sensor swath, thus resulting in much larger statistics (~ 3 million clear-sky nighttime pixels per 24-hour period), whereas the SNO is based on only a handful of match-up nadir looks per day. Also, DD statistics in MICROS are derived from deviations of clear-sky BTs and SSTs from their respective reference states, and follow narrow Gaussian distributions. On

the other hand, the SNO statistics are collected in all-sky conditions, in a wide range of illumination geometries, and over different types of underlying surface (ice, land, water). As a result, the SNO distributions are wide, strongly asymmetric, and scarcely sampled, making estimates of ensemble mean SNO biases less accurate. Unique to the DD technique is that it takes into account the difference in spectral response functions between the two sensors, whereas SNO measures a combined effect of sensor calibration and spectral response differences. Finally, since SNO are mostly collected in the polar areas, monitoring of Ch3B (3.7 μm) may be problematic during extended periods of polar days due to solar contamination. As shown in Fig. 6, the DD technique has no problem monitoring this band using nighttime ACSPO data.

Another implementation of the DD technique in GSICS is based on using measured (rather than RTM-modeled) high-resolution AIRS or IASI spectra and convoluting them with the sensor spectral response functions (e.g., *Hewison and König, 2008; Wang and Cao, 2008; Wang and Wu, 2008*). The wide-band sensor and the hyper-spectral instrument may be on the same platform (e.g. AVHRR and IASI on Metop-A, *Wang and Cao, 2008*) or the two instruments may be flown on different platforms. For example, imagers flown onboard MSG and MTSAT-1R geostationary satellites are evaluated against collocated IASI onboard Metop-A or AIRS onboard Aqua (*Hewison and König, 2008; www.eumetsat.int/Home/Main/DataProducts/Calibration/Inter-calibration/GSCISMeteosatIRInter-calibration/index.htm?l=en;%20http://mscweb.kishou.go.jp/monitoring/gsics/ir/gsir_mt1r.htm*).

Overall, the DD technique employed in MICROS is expected to be an effective supplement to the SNO methodology adopted in GSCIS for sensor inter-calibration.

5. Using MICROS analyses to validate and improve CRTM and input fields

MICROS analyses have been extensively employed to validate and improve CRTM. *Liang et al. (2009)* fine-tuned CRTM implementation in ACSPO. *Liu et al. (2009)* identified a deficiency in treatment of upper air data in CRTM r577 and fixed it in v1.1. Section 3.2 of this paper additionally demonstrated a small yet consistent improvement when PW coefficients were implemented in CRTM v1.1. *Liang et al. (2010)* employed MICROS to improve the solar reflectance model. As of this writing, the new and more accurate CRTM v2 was released to users. More recently, the CRTM team has tested improved transmission parameterizations in wide AVHRR bands, new versions of line-by-line (LBL) RTM, the effects of incorporating additional gases in the training data set, and the effects of Earth's curvature on M-O biases (*Chen and Han, 2010, personal communication*).

This section additionally demonstrates the value of MICROS to evaluate the effect of input SST field on the M-O biases. Analyses in section 3.1 have shown that using daily Reynolds SST, instead of weekly product, greatly improves global SDs between the first-guess BTs and SSTs and AVHRR observations. However, time series of BT and SST biases in Fig. 5 continue to exhibit significant and unexplained short- and long-term

spurious variations. Furthermore, anti-correlation between BT and SST biases is clearly apparent, suggesting that spurious variability in Reynolds SST is the cause.

To verify this observation, Fig. 7 (a) re-plots time series of M-O biases in Ch3B from Fig. 5 (b), zooming at the time interval from 1 January – 30 June 2009, which contained a large wave with the amplitude of several tenths of a kelvin. Note that median statistics are used in Fig. 7 to suppress the unwanted effects of possible outliers in ACSPO data and to emphasize the real trends in M-O biases. Also, unlike Fig. 5, each data point in Fig. 7 now represents one-day statistics (i.e., no seven-day smoothing is applied) to preserve day-to-day variations in both data sets. Corresponding temporal median and RSD statistics are superimposed. They show that typical RSDs $\sim 33 \pm 1$ mK. Fig. 7 (b) re-plots Fig. 7 (a) but using the UK Met Office daily OSTIA $1/12^\circ$ resolution foundation SST product (Stark et al., 2007), in place of daily 0.25° Reynolds SST, as CRTM input. There is no wave seen in the OSTIA time series, and RSDs have dramatically reduced to $\text{RSD} \sim 20 \pm 7$ mK.

Fig. 7 (c-d) shows corresponding times series of spatial RSDs, calculated within each individual day over the globe. Both Reynolds and OSTIA RSDs show non-uniformities in time, with respect to ACSPO SST. The fact that these non-uniformities are specific to Reynolds and OSTIA SSTs and not individual satellite SSTs suggests that they mainly come from these first-guess SSTs rather than from ACSPO product. On average, $\text{RSD} \sim 0.42$ K for Reynolds and ~ 0.32 K for OSTIA product, indicating that in addition to

being more stable in time, OSTIA also captures spatial SST variability better than Reynolds product.

Finally, the bottom panels in Fig. 7 compare the corresponding DDs. Non-uniformities in the time series of BTs seen in Fig. 7 (a-b) are expected to cancel out when calculating DDs. Comparisons between Fig. 7 (e) and Fig. 7 (f) suggest that indeed this cancellation largely takes place, but artifacts and noise in the DDs are still slightly smaller when OSTIA SST is used. The mean DDs are only slightly affected by the reference SST field.

Fig. 8 re-plots Fig. 7 but for SST biases. All observations seen in Fig. 7 continue to hold. The contrast between the Reynolds and OSTIA SSTs is larger than seen in Ch3B, as expected. With respect to foundation OSTIA SST, ACSPO nighttime SST is biased cold by $\sim 0.15 \pm 0.07$ K, close to the expected average skin-bulk difference (*Donlon et al., 2002*). The RSD ~ 0.47 K with respect to Reynolds and ~ 0.35 K with respect to OSTIA clearly indicate reduced spatial noise in the OSTIA SST using ACSPO SST as a “transfer standard.” Finally, DDs show that NOAA-18 SST is ~ 0.04 K cooler than NOAA-17, which is expected. However, warm biases in Metop-A and NOAA-19 SST are unexpected and suggest that MUT regression coefficients are suboptimal and should be re-derived for ACSPO.

6. Conclusions and future work

The MICROS Web-based tool was established to monitor global M-O biases in clear-sky brightness temperatures and SSTs over oceans in near-real time. MICROS is an end-to-end system that processes satellite Level 1B using ACSPO, performs statistical analyses of BTs and SSTs, and publishes their summaries on the Web. Currently, AVHRR BTs in Ch3B, 4, and 5 from NOAA-16, -17, -18, and Metop-A and regression SSTs are monitored. All analyses in MICROS are performed separately for day and night. Only more accurate nighttime data were used in this paper, as they are not contaminated by solar reflectance and only minimally affected by the diurnal cycle.

Generally, BT and SST biases are stable in time, even when ACSPO versions have changed. Residual short-term variations mostly arise from the instabilities in CRTM input fields, such as Reynolds SST. Using OSTIA SST as input significantly improves stability of BT and SST time series and reduces spurious spatial variability.

Cross-platform consistency is monitored using double differences. Typically, cross-platform biases are within several hundredths of a kelvin. These biases appear small, but in many cases they are statistically significant. Often, their magnitudes and signs are inconsistent with those expected based on diurnal variability (which is not accounted for in MICROS). In some cases the biases are quite large, such as in Ch4 of NOAA-18 and NOAA-19, which are biased cold relative to NOAA-17 and Metop-A by $\sim(0.10\pm 0.03)$ K and $\sim(0.14\pm 0.01)$ K, respectively. NOAA-16 is out-of-family and unstable.

Both conventional and robust statistics are implemented in MICROS. Robust statistics are more effective to evaluate the performance of sensor or CRTM and its input, whereas the conventional statistics are useful to evaluate the performance of the ACSPO product (e.g., *Merchant et al.*, 2008, 2009). Proximity of the two statistics is a good indicator of the product's overall well-being.

MICROS analyses revealed the need for improvement in several major areas. Daytime BTs are contaminated by the reflected solar signal, especially in the mid-IR Ch3B. Improved and physically justified surface reflectance model based on Cox-Munk formulation was implemented in CRTM version 2 (*Liang et al.*, 2010). It is now being tested and fine tuned, and the results will be reported elsewhere. Satellite radiances should be reconciled using the double-differencing technique, through improvements to sensor radiances (calibration and spectral response functions), and by accounting for the diurnal variability. We work closely with the CRTM team to explore global model aerosol fields (Goddard Chemistry Aerosol Radiation and Transport, GOCART, and Navy Aerosol Analysis and Prediction System, NAAPS) in conjunction with CRTM, to more accurately model TOA BTs and minimize M-O biases. The CRTM team constantly works to improve CRTM accuracy, and we keep exploring improved input fields (e.g., OSTIA versus Reynolds SST, and ECMWF upper air fields instead of GFS). Also, ACSPO SST and cloud mask algorithms are constantly evaluated and revisited. The effect of all these new improvements and developments is evaluated using the MICROS methodology.

Work is also underway to extend MICROS functionality to include monitoring of BTs from MSG/SEVIRI. Data from NPOESS/VIIRS and GOES-R/ABI will be added to MICROS once they become available.

Acknowledgements

This work is conducted under the Algorithm Working Group funded by the GOES-R Program Office, NPOESS Ocean Cal/Val project funded by IPO, and Polar PSDI and Ocean Remote Sensing Programs funded by NESDIS. CRTM is provided by the NESDIS Joint Center for Satellite Data Assimilation (JCSDA). Thanks to Yury Kihai for contribution in ACSPO granule collection, Feng Xu for helpful suggestions related to Web design, and Boris Petrenko for providing high-quality ACSPO clear-sky mask. Thanks also go to Quanhua Liu, Yong Han, Yong Chen, Paul Van Delst, Fuzhong Weng, Changyong Cao, Likun Wang, and Nick Nalli of NOAA/NESDIS for helpful discussions. The views, opinions, and findings contained in this report are those of the authors and should not be construed as an official NOAA or U.S. Government position, policy, or decision.

References

- Cao, C., M. Weinreb, and J. Sullivan, 2001: Solar contamination effects on the infrared channels of the advanced very high resolution radiometer, *J. Geophys. Res.*, **106**, 33,463–33,469, doi:10.1029/2001JD001051.
- Cao, C., J. Sullivan, E. Maturi, and J. Sapper, 2004a: The effect of orbit drift on the calibration of the 3.7 mm channel of the AVHRR onboard NOAA-14 and its impact on night-time sea surface temperature retrievals, *Int. J. Remote Sens.*, **Vol. 25**, pp. 975–986.
- Cao, C., M. Weinreb, and H. Xu, 2004b: Predicting simultaneous nadir overpasses among polar-orbiting meteorological satellites for the inter-satellite calibration of radiometers, *JTech*, **21**, 537–542.
- Chou, M. D., W. L. Ridgway, and M.-H. Yan, 1993: One-parameter scaling and exponential-sum fitting for water vapor and CO₂ infrared transmission functions, *J. Atmos. Sci.*, **50**, 2294–2303.
- Dash, P., and A. Ignatov, 2008, Validation of clear-sky radiances over oceans simulated with MODTRAN4.2 and global NCEP GDAS fields against nighttime NOAA15– 18 and MetOp-A AVHRRs data, *Remote Sens. Environ.*, **112**, 3012– 3029.
- Dash, P., A. Ignatov, Y. Kihai, and J. Sapper, 2010: The near real-time SST Quality Monitor (SQUAM). *JTech*, doi: 10.1175/2010JTECHO756.1, in press.
- Donlon, C. J., P. J. Minnett, P. J., C. Gentemann, T. J. Nightingale, I. J. Barton, B. Ward, and M. J. Murray, 2002: Toward improved validation of satellite surface skin temperature measurements for climate research. *J. Climate*, **15**, 353–369.

- Gentemann, C. L., and P. J. Minnett, 2008: Radiometric measurements of ocean surface thermal variability, *J. Geophys. Res.*, **113**, C08017, DOI: 10.1029/2007JC004540.
- Garand, L., 2003: Toward an integrated land-ocean surface skin temperature analysis from the variational assimilation of infrared radiances. *J. Appl. Meteor.*, **42**, 570–583.
- Han, Y., P. van Delst, Q. Liu, F. Weng, B. Yan, R. Treadon, and J. Derber, 2006: JCSDA Community Radiative Transfer Model (CRTM) – Version 1, *NOAA Technical Report NESDIS 122* [http://www.star.nesdis.noaa.gov/sod/sst/micros/pdf/CRTM_v1_NOAAtechReport-1.pdf]
- Harris, B.A., and G. Kelly 2001: A satellite bias correction scheme for radiance assimilation. *Quart. J. Roy. Meteor. Soc.*, **127**, 1453-1468.
- Hewison, T. J., and M. König, 2008: Inter-Calibration of Meteosat Imagers and IASI, *Proceedings of EUMETSAT Meteorological Satellite Conference*, Darmstadt, Germany, EUMETSAT P. 52, ISBN 978-92-9110-082-8. [http://www.eumetsat.int/Home/Main/AboutEUMETSAT/Publications/ConferenceandWorkshopProceedings/2008/SP_1232700911980?l=en]
- Ignatov, A., et al., 2004: Global operational SST and aerosol products from AVHRR: Current status, diagnostics, and potential enhancements, *13th AMS Conf. Satellite Oceanography and Meteorology*, AMS, Norfolk, VA. [<ams.confex.com/ams/pdfpapers/78049.pdf>]
- Köpken, C., G. Kelly, and J.-N. Thépaut, 2004: Assimilation of Meteosat radiance data within the 4D-Var system at ECMWF: assimilation experiments and forecast impact. *Q. J. R. Meteorol. Soc.*, **130**, 2277–2292.
- Kennedy, J. J., P. Brohan, and S.F.B. Tett, 2007: A global climatology of the diurnal variations in sea-surface temperature and implications for MSU temperature trends, *Geophys. Res. Lett.*, **34**, L05712, doi:10.1029/2006GL028920.

- Liang, X., A. Ignatov, and Y. Kihai, 2009: Implementation of the Community Radiative Transfer Model (CRTM) in Advanced Clear-Sky Processor for Oceans (ACSPO) and validation against nighttime AVHRR radiances, *J. Geophys. Res.* **114**, D06112, doi:10.1029/2008JD010960.
- Liang, X., A. Ignatov, Y. Han, and H. Zhang, 2010: Validation and improvements of daytime CRTM performance using AVHRR IR 3.7 μm band, *13th AMS Conf. Atm. Rad.*, 28 June - 2 July, [ams.confex.com/ams/pdfpapers/170593.pdf].
- Liu, Q, X. Liang, Y. Han, P. van Delst, Y. Chen, A. Ignatov, and F. Weng, 2009: Effect of Out-of-Band Response in NOAA-16 AVHRR Channel 3b on Top-of-Atmosphere Radiances Calculated with the Community Radiative Transfer Model, *JTech*, **26**, 1968–1972.
- May, D. A., M. Parmeter, D. Olszewski, and B. McKenzie, 1998: Operational processing of satellite sea surface temperature retrievals at the Naval Oceanographic Office, *Bull. Am. Meteorol. Soc.*, **79**, 397–407.
- McClain P., W. Pichel, and C. Walton, 1985: Comparative performance of AVHRR based multichannel sea surface temperatures, *JGR*, **90**, 11587–11601.
- Merchant, C., P. Le Borgne, A. Marsouin, and H. Roquet, 2008: Optimal estimation of sea surface temperature from split-window observations, *Remote Sens. Environ.*, **112**, 2469–2486.
- Merchant, C., P. Le Borgne, H. Roquet, and A. Marsouin, 2009: Sea surface temperature from a geostationary satellite by optimal estimation, *Remote Sens. Environ.*, **113**, 445–457.
- Munro, R., C. Köpken, G. Kelly, J.-N. Théapaut, and R. Saunders, 2004: Assimilation of Meteosat radiance data within the 4DVar system at ECMWF: data quality monitoring, bias correction, and single-cycle experiments, *Q. J. R. Meteorol. Soc.*, **130**, 2293–2313.
- Petrenko, B., A. Heidinger, A. Ignatov, and Y. Kihai, 2008: Clear-sky mask for the AVHRR Clear-Sky Processor for Oceans, *Ocean Sciences Meeting*, 2–7 March 2008, Orlando, FL.

[http://www.star.nesdis.noaa.gov/sod/osb/sst/ignatov/conf/2008-AGU-OSM-PetrenkoEtAl_ACSP0_CSM_Poster.pdf]

Petrenko, B., A. Ignatov, Y. Kihai, and A. Heidinger, 2010a: Clear-sky mask for the Advanced Clear Sky Processor for Oceans (ACSP0), *JTech*, doi:10.1175/2010JTECHA1413.1, in press.

[http://www.star.nesdis.noaa.gov/sod/osb/sst/ignatov/peer/PetrenkoEtAl-JTech-2010_ACSM.pdf]

Petrenko, B., A. Ignatov, and Y. Kihai, 2010b: Hybrid Algorithm for SST Retrieval: Combining Regression and Radiative Transfer Model Approaches. *JTech*, submitted.

[http://www.star.nesdis.noaa.gov/sod/osb/sst/ignatov/peer/PetrenkoEtAl-JTech-2010_Hybrid.pdf]

Reynolds, R. W., N. A. Rayner, T. M. Smith, D. C. Stokes, and W. Wang, 2002: An improved *in situ* and satellite SST analysis for climate, *J. Clim.*, **15**, 1609–1625.

Reynolds, R. W., T. M. Smith, C. Liu, D. B. Chelton, K. S. Casey, and M. G. Schlax, 2007: Daily high-resolution blended analyses for sea surface temperature. *J. Clim.*, **20**, 5473–5496.

Saunders, R., M. Matricardi, and P. Brunel, 1999: An improved fast radiative transfer model for assimilation of satellite radiances observations, *Q. J. R. Meteorol. Soc.*, **125**, 1407–1425, doi:10.1256/smsqj.55614.

Stark, J. D., C. J. Donlon, M. J. Martin, and M. E. McCulloch, 2007: OSTIA: An operational, high resolution, real time, global sea surface temperature analysis system. *OCEANS 2007 – Europe, IEEE Aberdeen*, DOI: 10.1109/OCEANSE.2007.430225.

Strow, L. L., S. Hannon, and D. Tobin, 2008: AIRS and IASI validation and inter-comparisons with SARTA, *Advanced High Spectral Resolution Infrared Observations Workshop*, EUMETSAT, Darmstadt, Germany, 15–17 September 2008.

[http://www.ssec.wisc.edu/hsr/meetings/2008/presentations/Larrabee_Strow.pdf]

- Stuart-Menteth, A.C., I.S. Robinson, and R.A. Weller, 2005: Sensitivity of the diurnal warm layer to meteorological fluctuations part 2: A new parameterization for diurnal warming. *J. Atmos. Ocean Sci.*, **10**, 209–234.
- Tobin, D., 2008: An SNO analysis of IASI and AIRS spectral radiance, *GSICS Quarterly*, **2**, 3 [http://www.star.nesdis.noaa.gov/smcd/spb/calibration/icvs/GSICS/documents/newsletter/GSICS_Quarterly_Vol2No3_2008.pdf]
- Turner, D., 2000: Systematic errors that are due to the monochromatic-equivalent radiative transfer approximation in thermal emission problems, *Appl. Opt.*, **39**, 5663–5670.
- Uddstorm, M. J., and L.M. McMillin (1994): System noise in the NESDIS TOVS forward model. Part I: Specification, *J. Appl. Meteor.*, **33**, 919-938.
- Wang, L, and C. Cao, 2008: On-orbit calibration assessment of AVHRR longwave channels on MetOp-A using IASI, *IEEE Trans. Geosci. Remote Sensing*, **46**, 4005–4013.
- Wang, L, and X. Wu, 2008: GSICS Tools Used to Compare IASI and AIRS, *GSICS Quarterly*, **2**, 4. [http://www.star.nesdis.noaa.gov/smcd/spb/calibration/icvs/GSICS/documents/newsletter/GSICS_Quarterly_Vol2No4_2008.pdf]
- Wu, A., X. Xiong, and C. Cao, 2008: *Terra* and *Aqua* MODIS inter-comparison of three reflective solar bands using AVHRR onboard the NOAA-KLM satellites, *Int. J. Rem. Sens.*, **29**, 1997–2010.

Table 1. Different versions of ACSPO employed in MICROS

	ACSPO v1.00	ACSPO v1.02	ACSPO v1.10
Time interval	1 Jul 2008 – 3 Sep 2008	4 Sep 2008 – 11 Nov 2008	12 Nov 2008 – 10 Oct 2009
Official version	Yes	No	Yes
CRTM version	R577	V1.1	V1.1
Ch3B coefficients	Ordinary	Planck-Weighted	Planck-Weighted
SST input to CRTM	Reynolds Weekly 1° OISST.v2	Reynolds Daily 0.25° ("AVHRR")	Reynolds Daily 0.25° ("AVHRR")
Cloud mask	Petrenko et al., 2008	Petrenko et al., 2010	Petrenko et al., 2010
Day/night flag (solar zenith angle)	85°	85°	90°

Figures

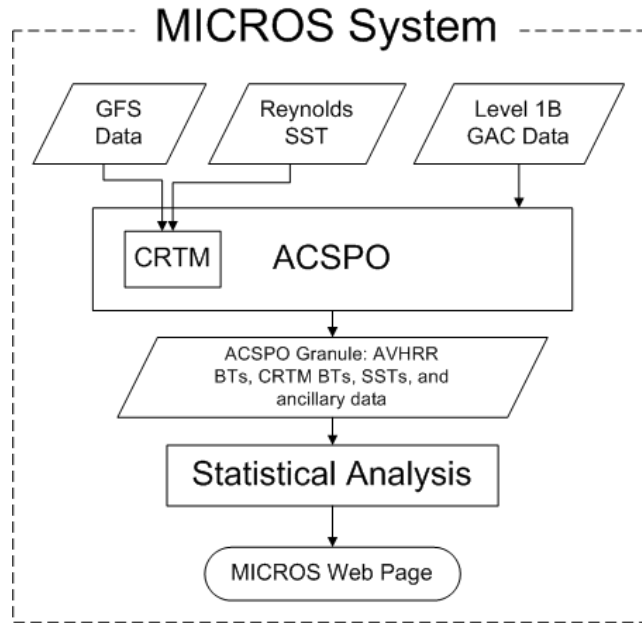


Figure 1. MICROS flow chart.

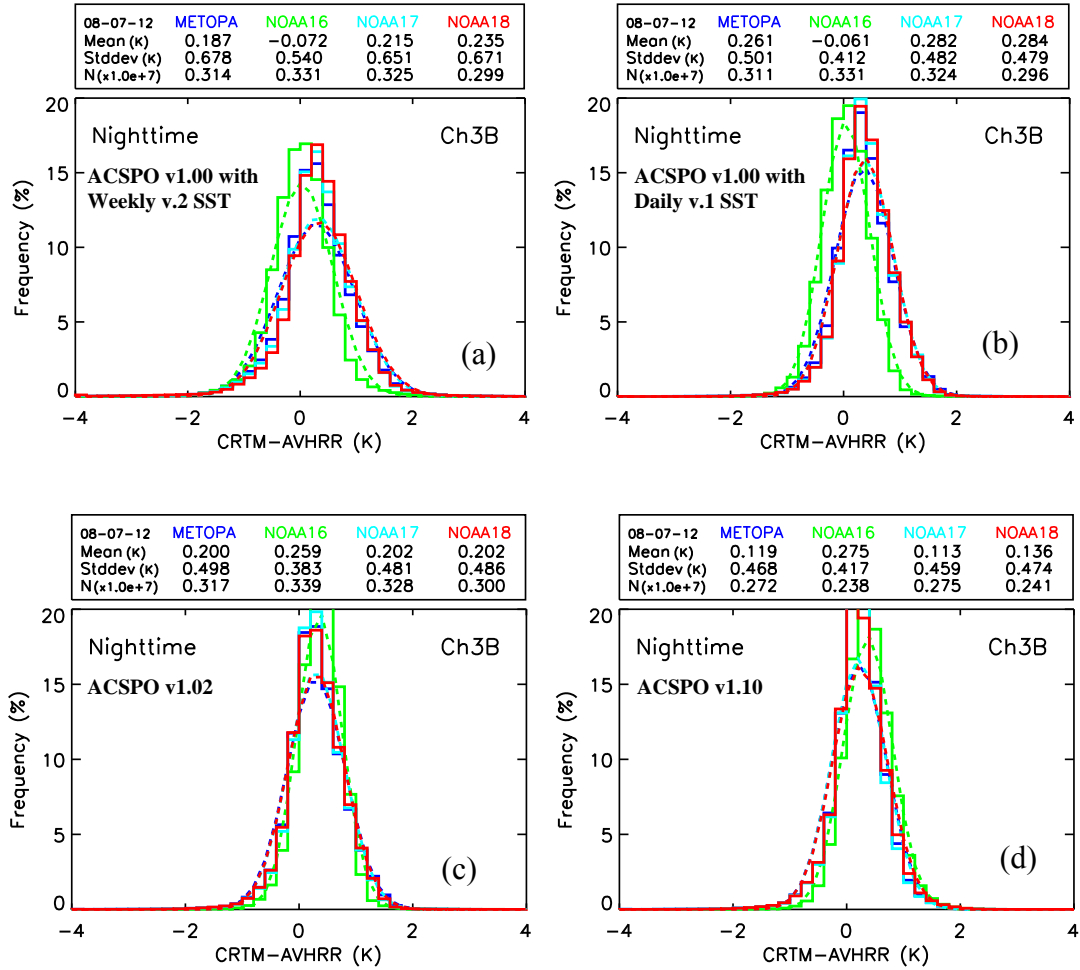


Figure 2. Global histograms of the M-O BT biases in AVHRR Ch3B onboard MetOp-A and NOAA16-18 for 24 hours of nighttime data for 12 July 2008. (a-b) ACSP0 v1.00 with (a) Reynolds weekly 1° v2.0 SST and (b) Reynolds daily 0.25° v1.0 SST (AVHRR-based) as CRTM input (CRTM r577 was used in both cases); (c) ACSP0 v1.02 (same as (b) but using CRTM v1.1 and Planck-weighted CRTM coefficients); (d) ACSP0 v1.10 (same as (c) but using upgraded cloud mask). The dot lines represent Gaussian distributions corresponding to the mean and standard deviation.

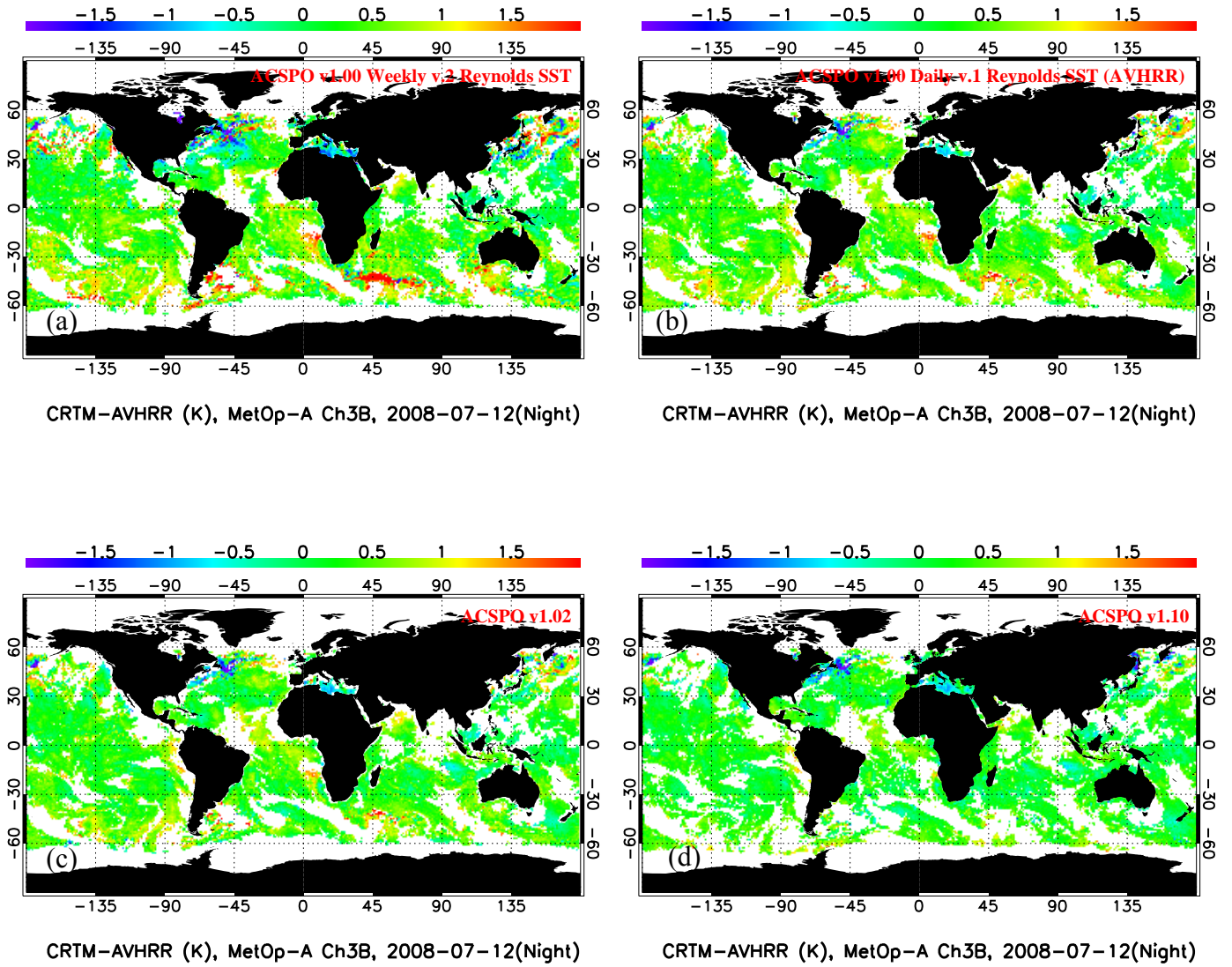


Figure 3. Geographical distribution of the M-O BT biases in MetOp-A Ch3B. Otherwise as in Fig. 1.

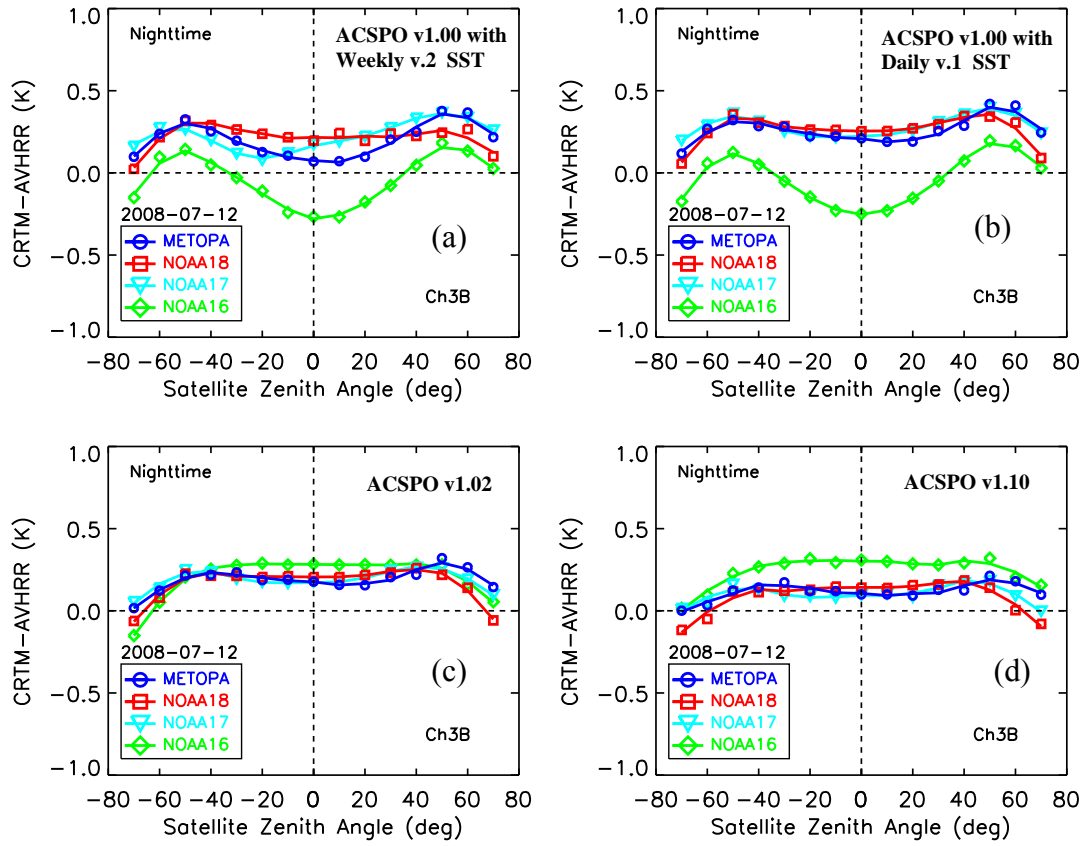


Figure 4. View zenith angle dependencies of the M-O BT biases. Otherwise as in Fig. 1.

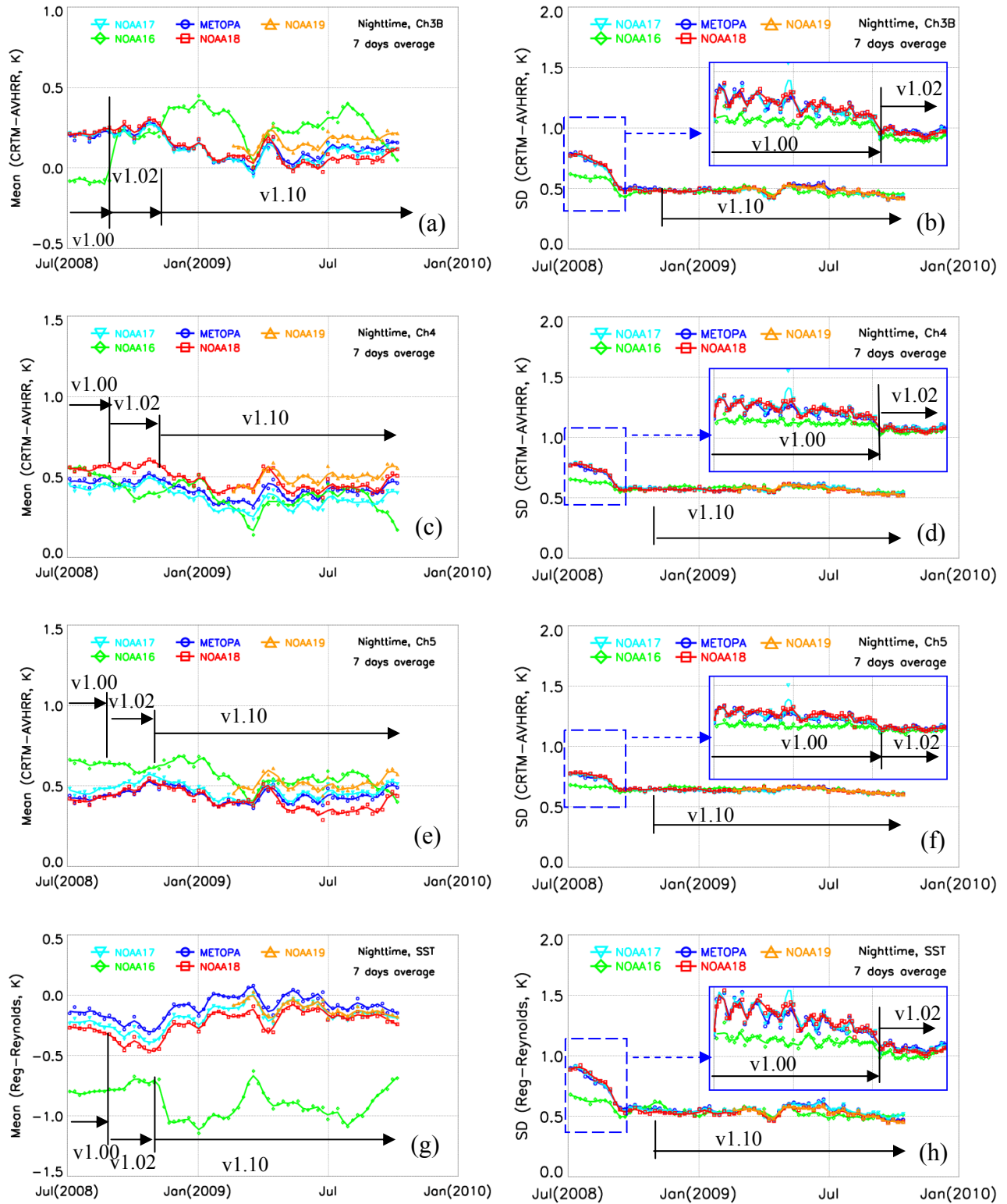


Figure 5. Time series of the global mean M-O biases and standard deviations (SD) for: (a, b) Ch3B; (c, d) Ch4; (e, f) Ch5; (g, h) SST. Each point in the graphs represents the statistics derived from all nighttime data with a seven-day smoothing. ACSPO versions are overlaid. The part fenced by the dash-line rectangle is magnified in the solid-line rectangle, where non-smoothed daily data are shown.

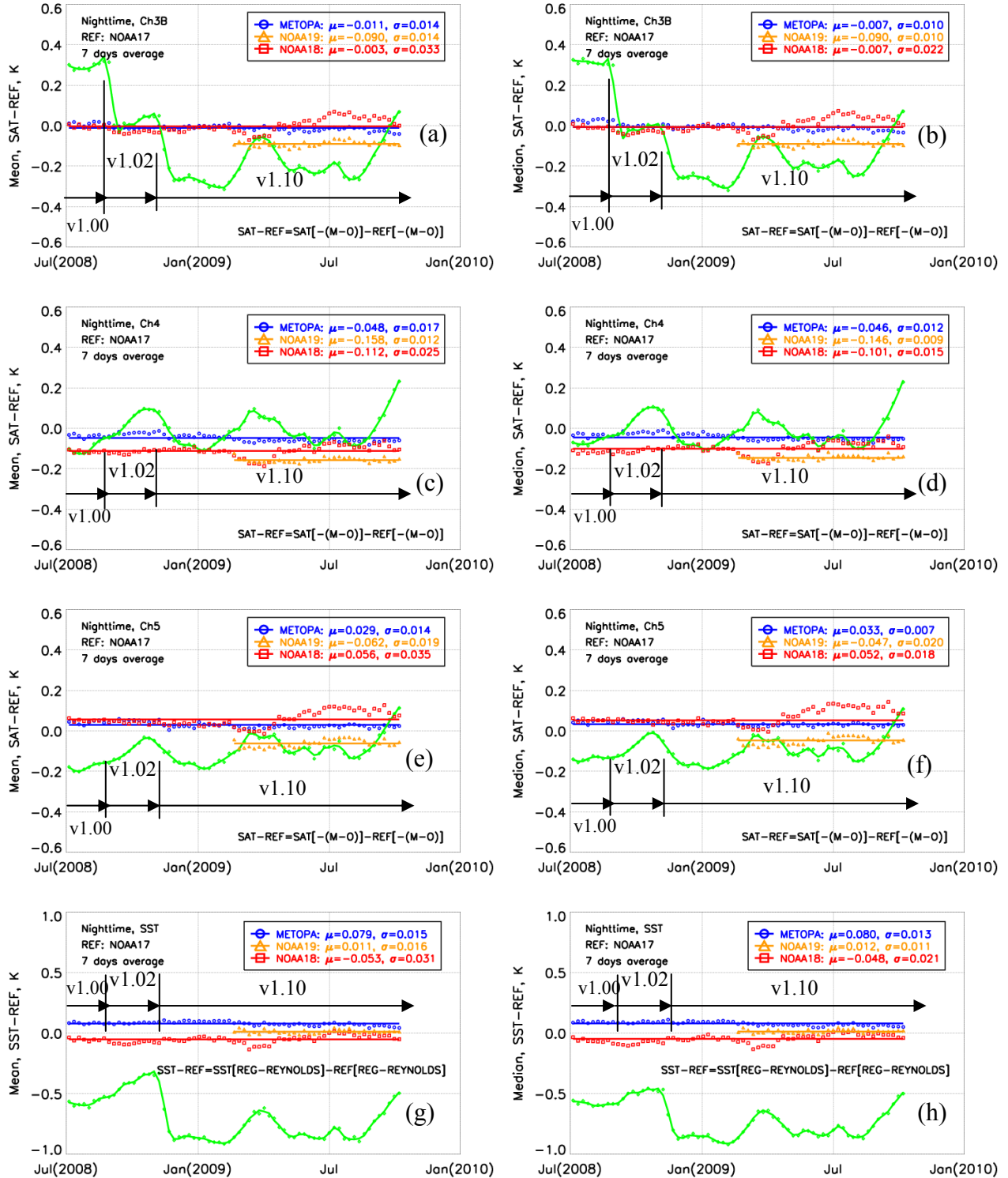


Figure 6. Cross-platform double-differences in AVHRR: (a, b) Ch3B, (c, d) Ch4, (e, f) Ch5, and (g, h) SSTs, using (a, c, e and g) mean and (b, d, f and h) median statistics. Data are smoothed out by a seven-day moving averaging filter to suppress noise and rectify signal. Mean and median values of the cross-platform biases and their corresponding day-to-day standard deviations are also shown.

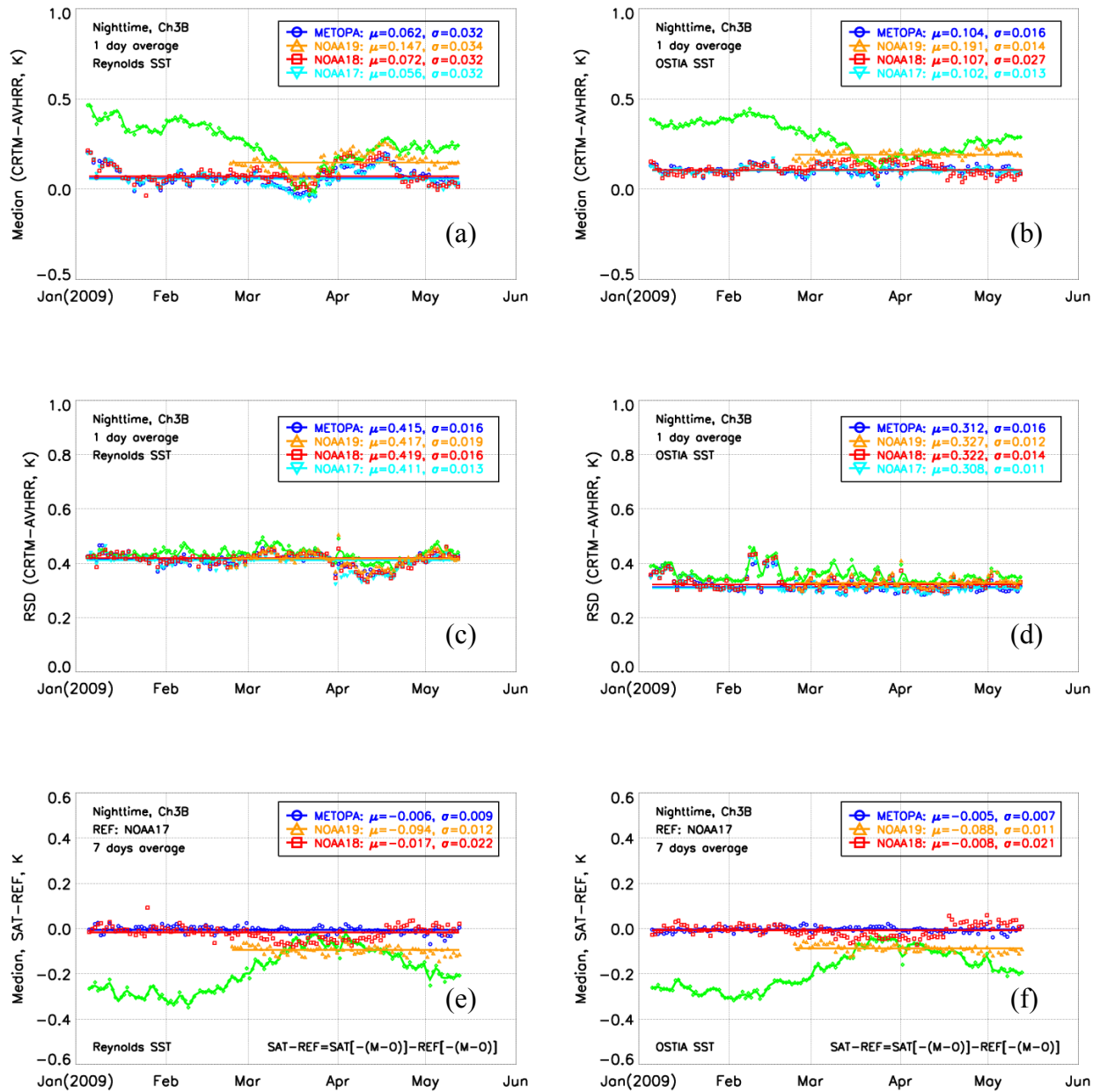


Figure 7. Time series of the global M-O median BT biases (a, b), RSD (c, d) and double differences (e, f) in AVHRR Ch3B for NOAA-16 through -19 and Metop-A calculated from ACSPO v1.10 using (a, c, e) Reynolds daily SST and (b, d, f) OSTIA SST as CRTM input. Each point in the graphs represents the statistics derived from all nighttime data within a 24-hour interval. The superimposed values of μ and σ represent median and RSD statistics derived from individual days.

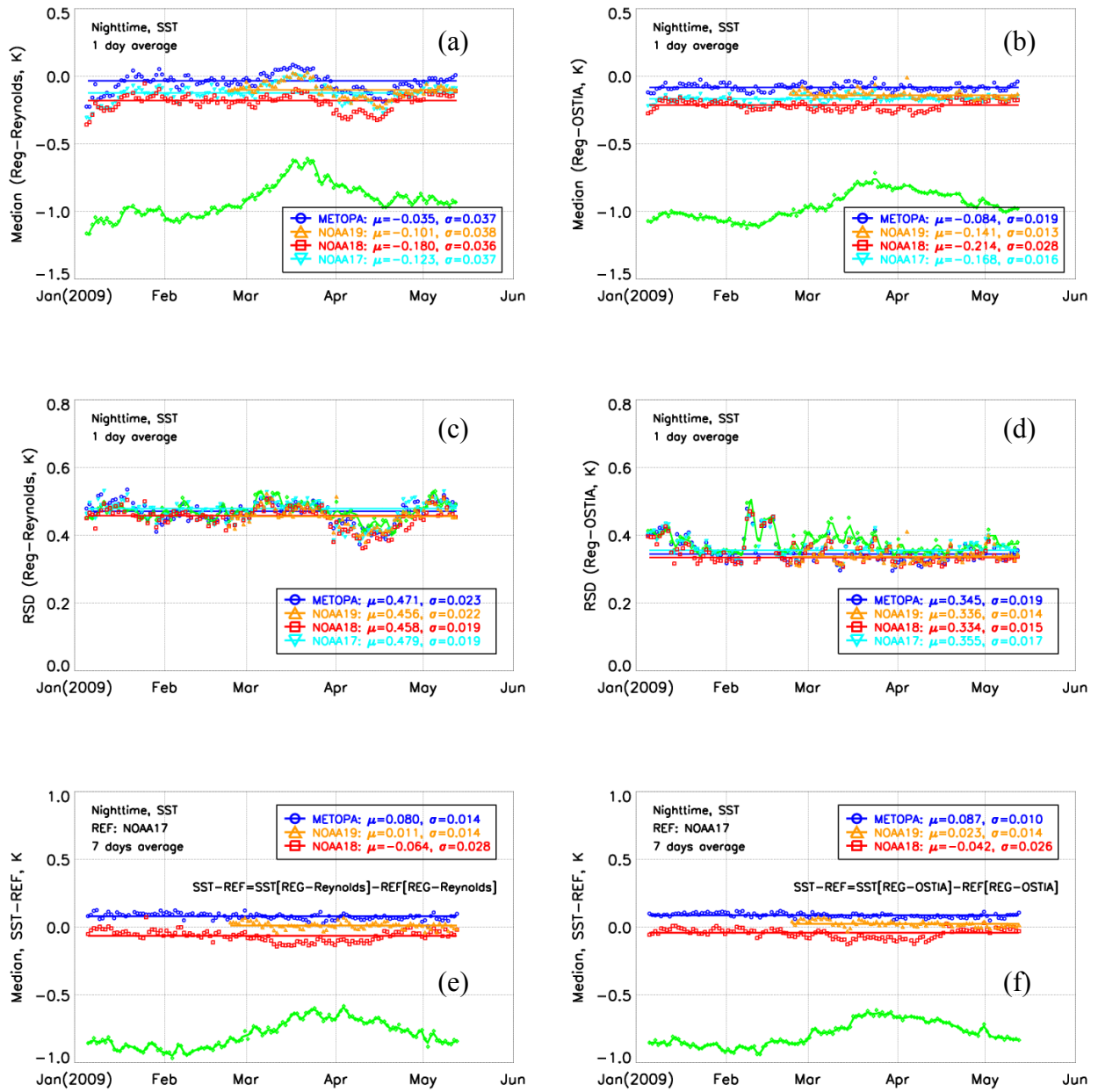


Figure 8. Same as in Fig. 7 but for global SST biases.